Induction of CD95 ligand expression on T lymphocytes and B lymphocytes and its contribution to apoptosis of CD95-up-regulated CD4$^+$ T lymphocytes in macaques by infection with a pathogenic simian/human immunodeficiency virus

Y. SASAKI, Y. AMI†, T. NAKASONE‡, K. SHINOHARA*, E. TAKAHASHI*, S. ANDO*, K. SOMEYA‡, Y. SUZAKI† & M. HONDA‡ *Department of Safety Research on Biologics, *Division of Biosafety Control and Research, †Division of Experimental Animal Research, and ‡AIDS Research Centre, National Institute of Infectious Diseases, Tokyo, Japan*

SUMMARY

Using an established SIV/HIV-C2/1-infected cynomolgus monkey model displaying stable CD4$^+$ T cell depletion, the kinetics of apoptosis and the levels of expression of CD95 membrane-associated CD95L on lymphocytes were investigated to test the involvement of the CD95/CD95L system in CD4$^+$ T lymphocyte loss *in vivo*. Rapid depletion of CD4$^+$ T cells occurred up to 2 weeks after infection, with chronic CD4$^+$ T lymphopenia thereafter. During the initial CD4$^+$ T cell loss, which was accompanied by viraemia, about 90% of the peripheral CD4$^+$ T cell subset underwent spontaneous apoptotic cell death during 24 h of culture. Increased expression of CD95 was observed on both CD4$^+$ and CD8$^+$ T cell subsets, with CD95 expression on CD8$^+$ cells declining rapidly, but high CD95 expression being maintained on CD4$^+$ cells. Since CD95L was expressed on CD8$^+$ T cells, B cells and to a lesser extent on CD4$^+$ T cells, this suggests that CD95-mediated apoptosis might be controlled in an autocrine/paracrine fashion.

Keywords simian/human immunodeficiency virus   CD4$^+$ lymphocyte depletion   apoptosis CD95   CD95 ligand

INTRODUCTION

HIV infection is a chronic disease associated with the deterioration of the immune system. The level of reduction in CD4$^+$ T lymphocyte numbers is the main indicator of the immunological state in patients with HIV. The mechanism of CD4$^+$ T cell depletion is not yet completely understood; however, several related phenomena have been described: (i) cross-linking of CD4 molecules on lymphocytes by gp120 of HIV and anti-gp120 antibody results in the death of the CD4$^+$ lymphocyte; (ii) both CD4$^+$ and CD8$^+$ T lymphocyte subsets from HIV patients die spontaneously through apoptosis in an *in vitro* culture system, and the magnitude of apoptosis correlates with the progression to immunodeficiency [1–4]; (iii) lymphocyte activation during the disease may be involved in the accelerated cell death.

Up-regulation of the expression of a cell surface receptor CD95 (Fas/APO-1), and its ligand CD95L, for the apoptotic signal is probably involved in the accelerated death of lymphocytes in HIV-infected individuals. CD95 expression on peripheral lymphocytes in HIV-infected subjects has been reported to increase

with disease progression [5,6]. Moreover, CD95 is expressed not only on memory cells but also on naive (CD45RA$^+$) cells in HIV infection [7,8], whereas it is expressed only on memory (CD45RO$^+$) cells in healthy donors [9]. In addition, spontaneous and anti-CD95 antibody-induced apoptosis in peripheral lymphocytes from HIV-infected subjects is reduced during highly active anti-retroviral therapy (HAART) [7,10]. The restoration of CD4$^+$ lymphocyte numbers during HAART is due to an increase in inactivated CD95$^-$ naive (CD45RA$^+$) CD4$^+$ T cells [11]. The involvement of CD95/CD95L-induced apoptosis during HIV infection is still controversial however, since no alteration in its levels has been detected during acute HIV infection following *in vitro* stimulation of lymphocytes with either phytohaemagglutinin (PHA) or phorbol myristate acetate (PMA)/ionomycin [12].

In a primate model, a link between the development of immunodeficiency and increased levels of apoptosis in CD4$^+$ T lymphocytes, associated with an increase in CD95 expression, has been reported [13,14]. On the other hand, resistance to anti-CD95 antibody-induced apoptosis in HIV-infected asymptomatic chimpanzees suggests that other apoptosis-related molecules are important [15]. These primate models mainly investigated the chronic phase of virus infection, and the question of the involvement of the CD95/CD95L system in both HIV replication and CD4$^+$ cell depletion remains open. A kinetic analysis of

lymphocyte apoptosis by Reinberger *et al.* [16] suggested a correlation between apoptosis in both $CD4^+$ and $CD8^+$ T cell populations and infection with an SIV/HIV hybrid virus (SHIV). Recently, we established a highly pathogenic SHIV-infected cynomolgus monkey model which displayed rapid $CD4^+$ lymphocyte depletion within 2 weeks, coinciding with an increase in the plasma viral load [17]. The very low peripheral $CD4^+$ T cell level persisted for at least 3 months after infection. In the present study, we investigated the spontaneous apoptotic level in cultured peripheral blood mononuclear cells (PBMC), and the expression of CD95 and CD95L on lymphocytes, in these SHIV C2/1-infected macaques in order to clarify the role of the CD95/CD95L system in the rapid decline in $CD4^+$ T lymphocyte numbers.

MATERIALS AND METHODS

Macaque and virus

Cynomolgus monkeys bred at the Tsukuba Primate Research Centre in the National Institute of Infectious Diseases, Japan were used. The original SHIV strain was kindly provided by Dr Y. Lu at the Virus Research Institute (Cambridge, MA) [18,19]. In our laboratory, the strain was infected *in vivo* by passages through two cynomolgus monkeys [17]. The SHIV C2/1 strain was intravenously inoculated with 20 TCID doses into eight cynomolgus monkeys, and peripheral blood was routinely drawn during the experimental period.

Analysis of cell surface molecules and determination of cell counts

Monoclonal antibodies against anti-human CD4 (NU-Th/1, mouse-IgG1; Nichirei Corp., Tokyo, Japan), CD8 (NU-Ts/c, mouse-IgG2a; Nichirei), HLA-DR (NU-Ia, mouse-IgG2a; Nichirei), CD95 (DX2, mouse-IgG1; PharMingen, San Diego, CA) and CD95L (4H9, hamster-IgG; MBL Corp., Nagoya, Japan) were used for analysis. Either anti-mouse IgG1 or IgG2a (Becton Dickinson Immunocytometry System, San Jose, CA) was used as the isotype-matched control antibody. All MoAbs, except anti-CD95L MoAb, were directly conjugated with FITC, PE or peridinin chlorophyll protein (PerCP). For CD95L, FITC-labelled anti-hamster IgG (Southern Biotechnology Associates, Inc., Birmingham, AL) was used as the second antibody.

Peripheral leucocytes were isolated from fresh blood after lysis of erythrocytes with erythrocyte lysis buffers (150 mM ammonium chloride, 9·9 μM potassium hydrogen carbonate and 99·3 mM EDTA-2Na). The cells were stained on ice first by FITC-conjugated MoAbs, second by PE-conjugated MoAbs and third by PerCP-conjugated MoAbs for 15 min each. For CD95L staining, the metalloprotease inhibitor KB-R8301, which was a gift from Kanebo Ltd (Osaka, Japan), was added at a concentration of 10 mM to inhibit cleavage of the membrane-bound CD95L to its soluble form. Three-coloured staining was performed for only two of the eight monkeys (no. M-6 and no. M-7).

For the absolute count, 50 μl of each whole blood sample containing FITC-conjugated anti-CD3 MoAb (BioSource Int. Inc., Camarillo, CA), PE-conjugated anti-CD4 MoAb (Becton Dickinson Immunocytometry System) and PerCP-conjugated anti-CD8 MoAb (Becton Dickinson Immunocytometry System) were added to a 12 × 75 mm polystyrene round-bottomed tube (Becton Dickinson Immunocytometry System), which was then incubated at 4°C for 15 min. Erythrocytes were then lysed by FACS lysing solution (Becton Dickinson Immunocytometry System) at 4°C for

15 min, and 50 μl of Flow-Count™ (Beckman Coulter Inc., Hialeah, FL) were added to each tube. The stained cells were analysed by FACScalibur flow cytometry (Becton Dickinson Immunocytometry Systems) using the software CellQuest (Becton Dickinson Immunocytometry System) after fixation with 1% paraformaldehyde.

Measurement of apoptosis in PBMC

PBMC were isolated from fresh blood by centrifugation using Percoll with a specific gravity of 1·070. PBMC (1×10^6) were then cultured for 18 h in RPMI medium containing 10% (v/v) heat-inactivated fetal calf serum, penicillin G 50 U/ml, streptomycin 50 μg/ml, and L-glutamine 1 mM. The apoptotic nuclei were quantified by a modification of a method described by Nicoletti [20]. Briefly, 1×10^6 cells, after centrifugation at 200 *g* to form a pellet, were suspended in 1 ml of a propidium iodide (PI)/Triton solution (PI 50 μg/ml in 0·1% Triton-x 100 plus 0·1% sodium citrate) and stored at 4°C in the dark overnight. The PI fluorescence of the nuclei was measured by a flow cytometer (FACScalibur) using CellQuest software. Cell debris was excluded by gating with forward scatter (cell size) and side scatter (granulosity) criteria. The DNA peaks of apoptotic nuclei could be identified below the G_0/G_1 cell cycle diploid peak. To quantify the apoptotic cells in either the $CD4^+$ or $CD8^+$ T cell subset, the 7-amino actinomycin D (7AAD; Sigma Chemical Co., St Louis, MO) incorporation method was performed. By staining with 20 μg/ml of 7AAD, after previously blocking with 20 μg/ml of non-fluorescent actinomycin D (Sigma), the fluorescence of apoptotic cells is increased compared with non-apoptotic cells due to the alteration in membrane permeability. $7AAD^+$ cells were counted as apoptotic cells by FACS.

Histochemical analysis of apoptosis in lymph nodes

Terminal deoxynucleotidyl transferase (TdT)-positive apoptotic cells were investigated histologically in lymph nodes from an SHIV-C2/1-infected cynomolgus macaque. The infected macaque was killled 11 days after infection, and paraffin-embedded lymph nodes were analysed using the TUNEL method (Apoptag™; Oncor, Gaithersburg, MD).

Measurement of plasma viral load of SHIV

Plasma viral RNA was extracted and purified using the QIAamp Viral RNA Mini Kit (Qiagen, Valencia, CA). For quantitative analysis of the RNA, the TaqMan™ system (PE Biosystems, Foster City, CA) was used with primers and probes targeting the SIVmac239 gag region, designed by computer with the Primer Express software (PE Biosystems). The viral RNA was amplified using TaqMan™ EZ RT-PCR Kit (PE Biosystems) with the designed primers (forward primer AATGCAGAGCCCCAAGAAGAC; reverse primer GGACCAAGGCCTAAAAAACCC) and detected by the probe Fam-ACCATGTTATGGCCAAATGCC-CAGAC-Tamra. The reverse transcriptase-polymerase chain reaction (RT-PCR) product was quantitatively monitored by its fluorescent intensity with ABI7700 (PE Biosystems). As control RNA, SIVmac239 gag RNA was synthesized and purified using MEGAscript™ (Ambion, Austin, TX) with a template plasmid pKS460 that contains SIVmac239 gag under the T7 promoter. Plasma viral load, which was measured in duplicate, was calculated based on the standard curve of control RNA and RNA recovery rate.

RESULTS

Correlation of CD4$^+$ T cell decline with increased apoptosis in PBMC in cynomolgus macaques infected with SHIV-C2/1 strain

Marked CD4$^+$ T cell depletion was observed in all macaques tested during the 2 weeks after virus infection. Figure 1a shows data from four macaques. The CD4$^+$ T lymphopenia was maintained during the 90-day observation period. Although there was a temporary decrease in CD8$^+$ T cell numbers within 10 days after infection, the number of CD8$^+$ T cells had recovered by 3 weeks.

To determine whether apoptosis caused the CD4$^+$ T cell depletion, the levels of spontaneous apoptotic cells at varying time points after infection were investigated by 24 h culture of monkeys' PBMC (Fig. 1b). The peak of apoptosis in PBMC, which occurred 11–17 days post-inoculation, coincided with the time of CD4$^+$ T cell loss. Apoptosis in both CD4$^+$ and CD8$^+$ T cell subsets was at a maximum coincidentally with both CD4$^+$ T cell loss and with the increase in spontaneous apoptosis of PBMC, and at the peak about 90% of CD4$^+$ cells were apoptotic (Fig. 1c).

Viral load in macaques infected with SHIV-C2/1

As shown in Fig. 1d, and in accordance with our previous work, plasma viral load peaked about 12 days after infection, with
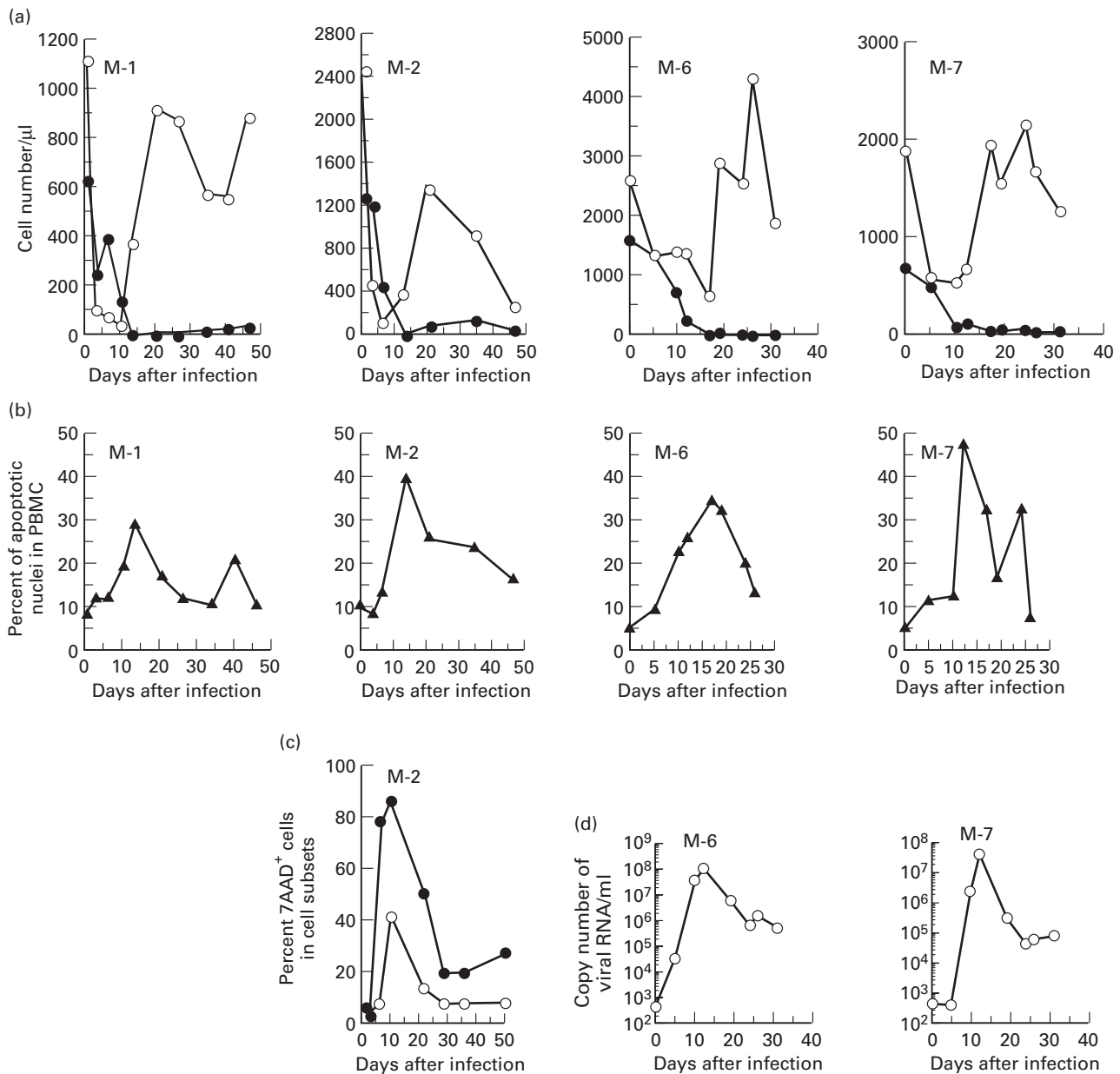

Fig. 1. Kinetic analysis of (a) absolute cell count of lymphocyte subsets, (b) apoptotic cell rate in peripheral blood mononuclear cells (PBMC), (c) apoptotic cell rate in T lymphocyte subsets, and (d) plasma viral load in SHIV-C2/1-infected macaques. Data from each individual macaque infected with SHIV-C2/1 are indicated (M-number). (a) ●, ○, absolute counts of CD4$^+$ or CD8$^+$ T lymphocytes in peripheral blood, respectively. (b) ▲, Percentage of apoptotic cells in PBMC cultured for 24 h. (c) ●, ○, percentage of apoptotic cells in the CD4$^+$ or CD8$^+$ T lymphocyte subsets, respectively. (d) ○, Copy number of viral RNA/ml of plasma. 7AAD, 7-amino actinomycin D.

$> 5 \times 10^7$ copies/ml. After the initial peak, the viraemia was maintained around 1–10×10^5 copies/ml.

Apoptosis in lymph nodes during severe CD4+ T lymphopenia

To study whether apoptosis was induced in lymphoid tissues of macaques by SHIV-C2/1 infection, one macaque (no. M-8) was killed 11 days after inoculation when CD4+ T cell depletion was apparent (i.e. CD4+ T cells composed only 4% of the total T lymphocytes; Fig. 2a). As shown in a lymph node section (Fig. 2b), the submandibular lymph nodes were swollen and hyperplastic when stained with H–E. Using TUNEL analysis, a few cells with fragmented TdT+ nuclei were clearly detected in the paracortex (Fig. 2Bii) and in the follicles of the lymph node (Fig. 2Biv). Similarly, TdT+ apoptotic cells were also detected in the paracortical area in axillary, inguinal and mesenteric lymph nodes (data not shown). By contrast, TdT+ cells were only detected in the centre of follicles in nodes from uninfected macaques (Fig. 2c).

Expression of CD95 on T lymphocytes in macaques infected with SHIV-C2/1

Since previous work showed that CD95 is more strongly expressed on T lymphocytes in AIDS patients than in HIV-infected asymptomatic persons, we investigated whether the CD95/CD95L system contributed to the depletion of CD4+ T lymphocytes in this macaque model. The percentages of CD95+ cells in each T cell subset from the seven macaques are shown in Fig. 3b. The magnitude of CD95 expression on both CD4+ and CD8+ T cells, measured by mean fluorescence intensity (MFI), started to increase 3 days after infection. The initial high peak of CD95 expression on both CD4+ and CD8+ T cells was detected 11–17 days post-inoculation, which coincided with CD4+ T cell depletion as shown in Fig. 3a. The pattern of CD95 expression was different in CD4+ and CD8+ T cells. First, at the peak, CD95 expression on CD4+ T cells was more than three to four times higher than the level in animals before infection, and was more intense than that on CD8+ cells. Second, CD95 expression on CD8+ cells gradually decreased after the peak, but persisted at a high or increased MFI level on CD4+ cells.

Expression of membrane-bound CD95L on lymphocytes in macaques infected with SHIV-C2/1

To investigate the CD95L signal responsible for the induction of apoptosis in CD95-expressing T lymphocytes, the expression of membrane-bound CD95L on the surface of PBMC was analysed. As shown in Fig. 3c, CD95L expression on CD8+ T cells started to increase from the very early phase of virus infection. On the other hand, although the percentage of CD95L+ cells in the CD4+ T cell subset was much lower than that in CD8+ T cells, increased expression of CD95L on CD4+ T cells was detected in four of the seven macaques, especially in the M-7 monkey. A small increase in expression of one of the T cell activation markers, HLA-DR, was detected in CD8+ cells, and in some cases HLA-DR expression appeared to coincide with CD95L expression (Fig. 3d, . 4c). By triple staining in the M-6 monkey 12 days after virus infection (Fig. 4a–e), more CD95 molecules in the CD8+ T cell subset were found to be expressed on HLA-DR+ (MFI = 217) than HLA-DR− cells (MFI = 128) (Fig. 4d). In the same monkey, expression of CD95L molecules was also higher on HLA-DR+ (MFI = 33) than HLA-DR− CD8+ T cells (MFI = 22) (Fig. 4e). In addition, membrane-bound CD95L expression was also

detected by triple staining in HLA-DR+ CD4−CD8− lymphocytes. Most of the cells in this population are B cells, as confirmed by being positive for CD20 (Fig. 4f). Kinetic analysis of CD95L on B cells is shown in Fig. 3e, and CD95L expression on B cells also peaked 10–12 days after virus infection (43% and 92% in nos M-6 and M-7, respectively), coinciding with CD95L expression on T lymphocytes. For monocytes, >90% of the CD14+ cells were CD95L+ regardless of viral infection (data not shown).

DISCUSSION

In this monkey model, the rapid CD4+ T cell decline in the acute phase of virus infection was associated with SHIV viraemia, since CD4+ T cells disappeared, and apoptotic cells in PBMC increased (30–50% of PBMC), around the time of the initial peak of viraemia in all monkeys investigated. As we previously described [17], the initial peak of viraemia occurs 12 days after infection, and plasma antigenaemia (as detected by SIV p27 antigen ELISA at that time) was $15\,000 \pm 3366$ pg/ml in all seven cynomolgus monkeys infected with 20 TCID$_{50}$ SHIV-C2/1, including five monkeys which we describe in this paper (nos M-1, 2, 3, 4 and 5). The plasma viral load, as measured by quantitative RT-PCR in two monkeys (M-6 and M-7), also showed that the initial peak of viraemia occurred 12 days after infection, with $> 5 \times 10^7$ viral RNA copies/ml. These data suggest an involvement of either HIV replication or viral products in the induction of lymphocyte death.

The CD95/CD95L associated pathways of apoptosis are multifactor signal cascades acting through cytoplasmic caspase activity, release of cytochrome c from mitochondria, activation of caspase-activated DNase (CAD) and translocation of CAD into the nucleus. The CD4+ T cell loss in our monkey model is initially rapid until 14–20 days after infection (first phase), followed by stable low levels of depletion (second phase). During the first phase, in agreement with previous observations [8,21], the increase in CD95 expression was not restricted to CD4+ T cells; however, CD95+CD8+ T cells disappeared in the second phase, in contrast to the strong expression of CD95 on CD4+ T cells. This suggests that the continuous high level of CD95 expression on CD4+ T cells (at an MFI > 200) resulted in the failure of recovery of CD4+ cell count during infection. In humans, HAART restores the early decline in the CD4+ T cell count which is paralleled with a rise in CD95− naive CD4+ T cells and a decrease in anti-CD95 antibody-induced apoptosis in PBMC *in vitro* [7,11].

Lymphocyte activation could contribute to the induction of both CD95 and CD95L expression on the surface of cells, as stronger expression of CD95L on activated, compared with unactivated, CD8+ T cells was detected. Others have shown that HIV-tat induces B cell hyperactivation *in vitro*, including CD95 expression, although CD95L expression was not analysed because of spontaneous expression in the culture system [22]. Our results agree with other reports of high levels of CD95L on peripheral human B lymphocytes in HIV-infected individuals, which is probably responsible for the induction of apoptosis [23]. In the case of Epstein–Barr virus infection, it is known that the virus induces CD95 expression on T cells, and CD95L expression on B cells, leading to T cell apoptosis [24]. In HIV infection and SHIV infection model, apoptosis occurs not only in CD4+ cells but also in CD8+ cells and B cells [25]. The presence of apoptotic cells in both the T and B cell areas in monkey lymph nodes we observed may be a reflection of hyperactivation during the initial viraemia.

For monocytes, positive staining for CD95L in CD14+ cells (> 90%) was consistently obtained regardless of the presence of
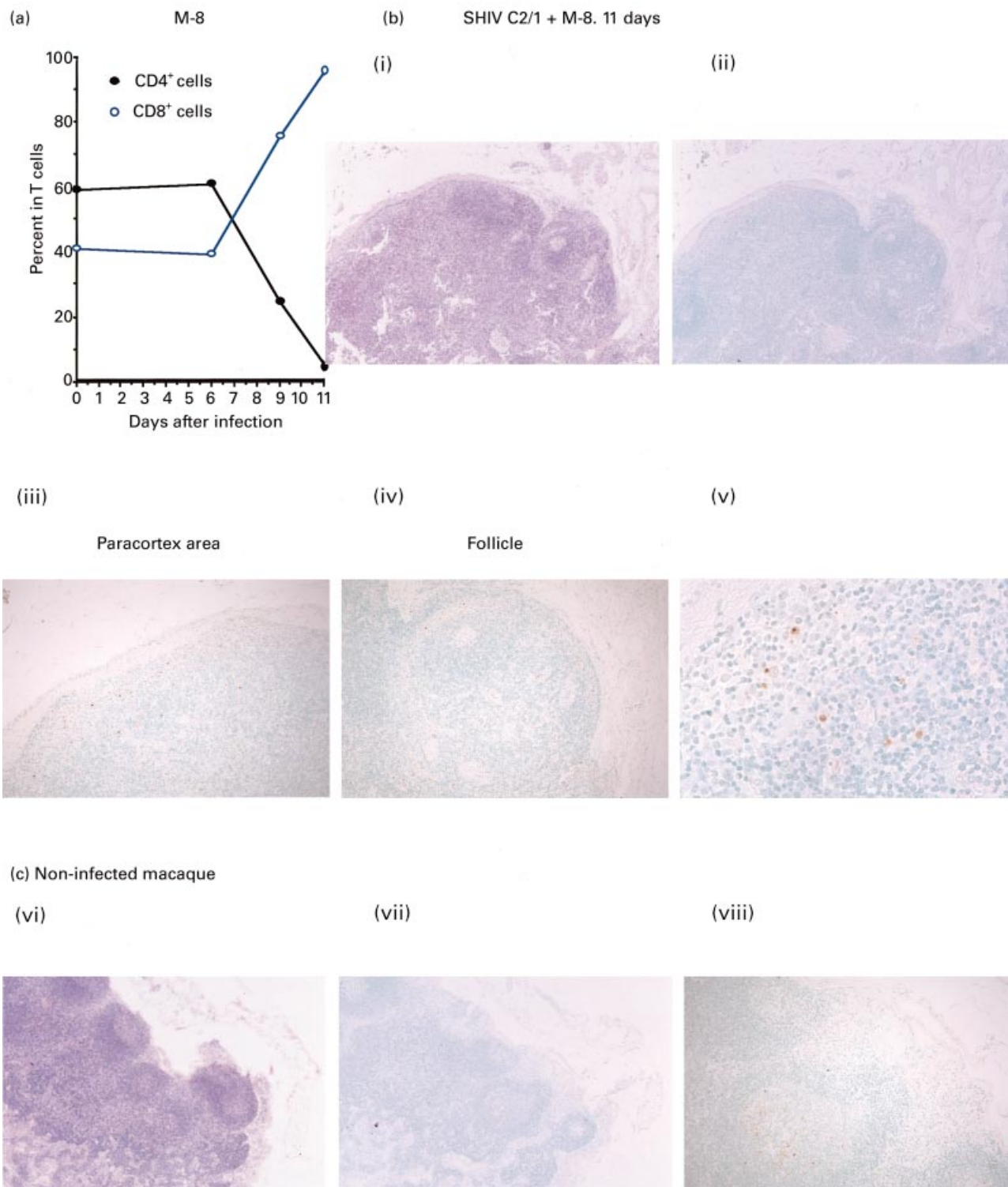
Fig. 2. Histological analysis of TdT$^+$ apoptotic cells by the TUNEL method in a submandibular lymph node from an SHIV-C2/1-infected macaque at day 11 post-inoculation. (a) Changes in percentage of either CD4$^+$ or CD8$^+$ cells in T lymphocytes in one representative monkey. (b) Detection of TdT$^+$ cells in a lymph node from an SHIV-C2/1-infected macaque at day 11 post-inoculation. Both Bi and Bii show images of a section of lymph node, Biii shows a magnified image in the paracortex area, and Biv and Bv show magnified images of follicles in the lymph node. (c) TUNEL staining of a submandibular lymph node obtained from an uninfected control animal. Haematoxylin and eosin (Bi and Cvi, mag. × 40), TUNEL (Bii, mag. × 40; Biii and Biv, mag. × 100; Bv, mag. × 400; Cvii, mag. × 40, and Cviii, mag. × 100) staining procedures were used.
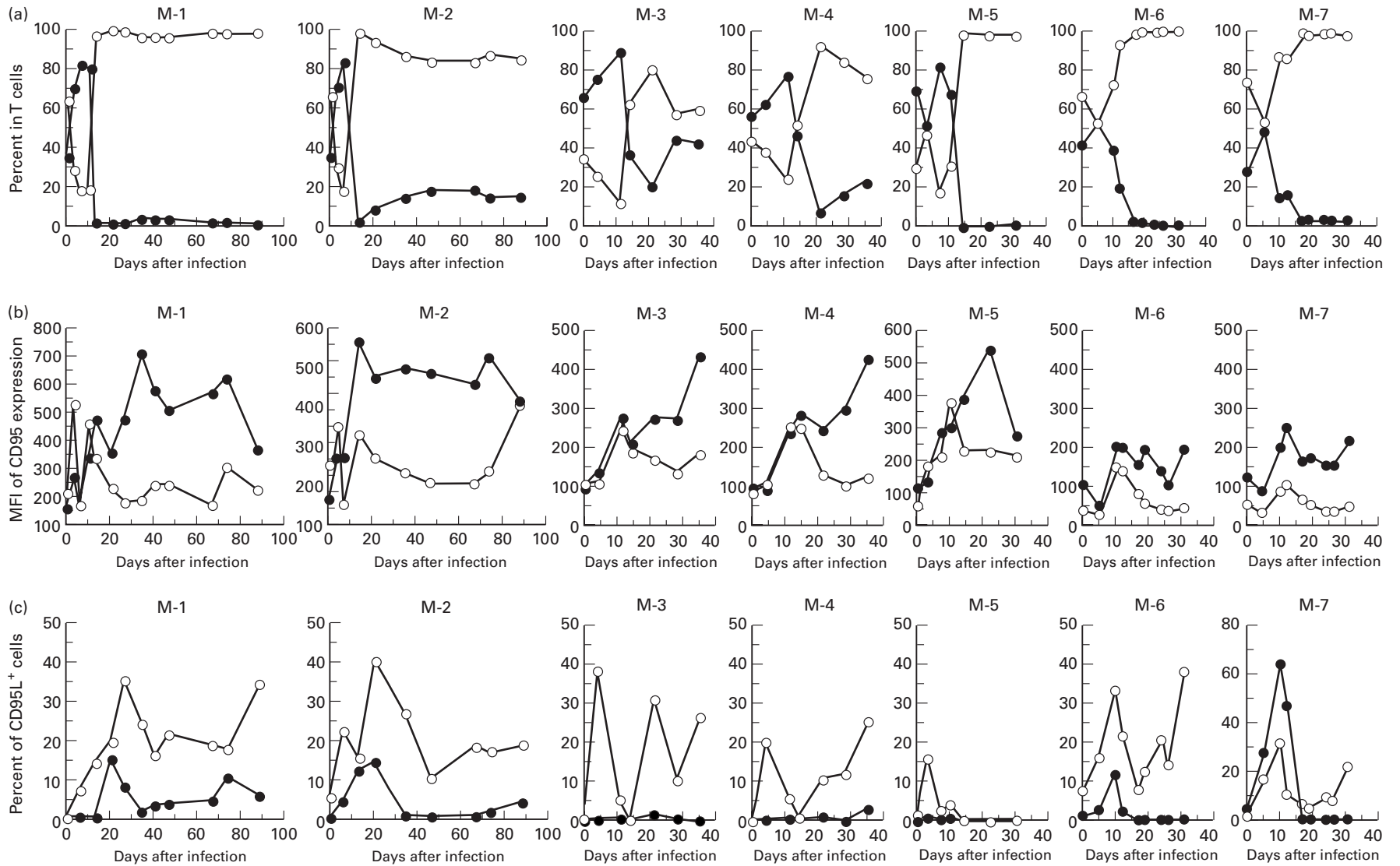
Y. *Sasaki* et al.

Fig. 3. Kinetic analysis of the distribution of cell subsets in T lymphocytes and CD95, CD95L or HLA-DR expression on the lymphocyte subsets from SHIV-C2/1-infected macaques (nos M-1–7). Each figure indicates kinetic data from an individual macaque (M-number). (a–d) ●, ○, CD4+ or CD8+ T cells, respectively. (a) The percentage of CD4+- or CD8+-expressing cells in T lymphocytes; (b) the mean fluorescence intensity (MFI) of CD95 expression; (c) percentage of C95L-expressing cells; and (d) the percentage of HLA-DR-expressing cells are shown; (e) percentage of CD95L (■)-expressing cells in B cells.
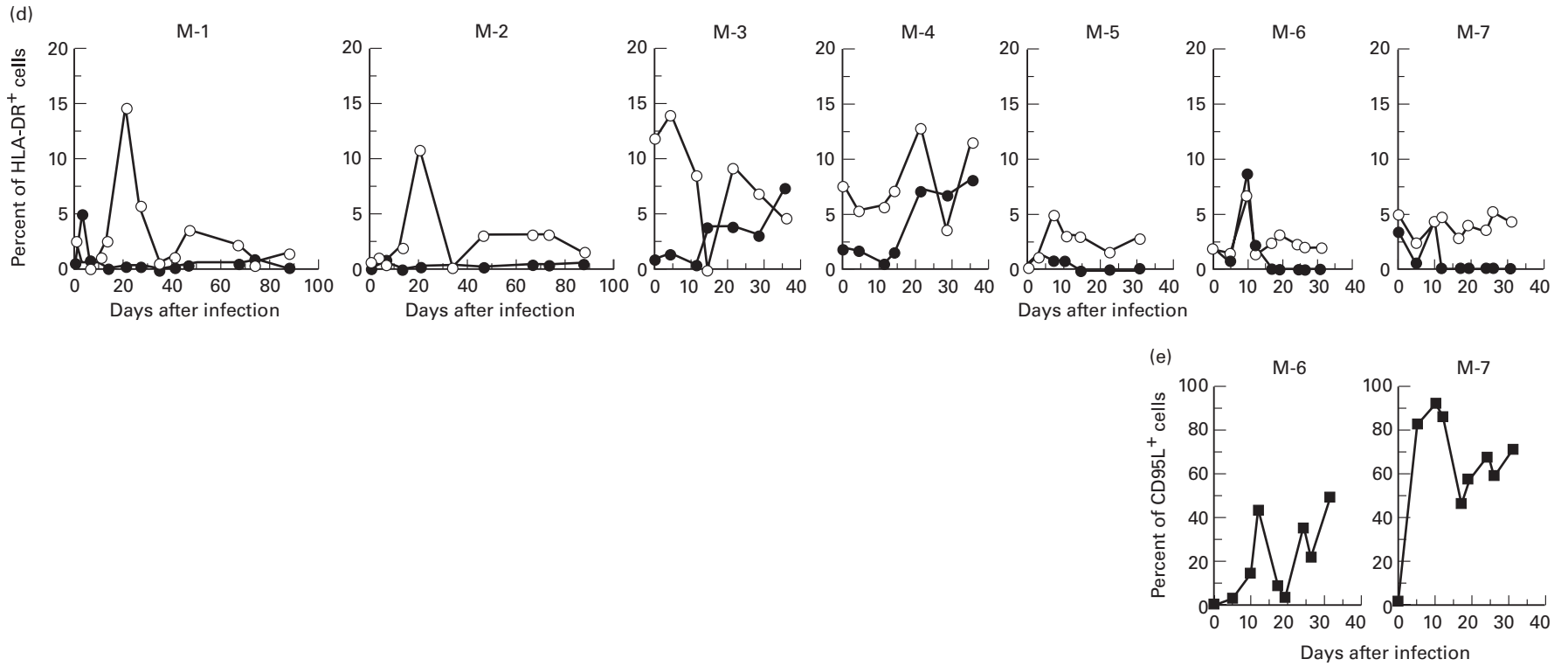
Fig. 3. Kinetic analysis of the distribution of cell subsets in T lymphocytes and CD95, CD95L or HLA-DR expression on the lymphocyte subsets from SHIV-C2/1-infected macaques (nos M-1–7). Each figure indicates kinetic data from an individual macaque (M-number). (a–d) ●, ○, CD4$^+$ or CD8$^+$ T cells, respectively. (a) The percentage of CD4$^+$- or CD8$^+$-expressing cells in T lymphocytes; (b) the mean fluorescence intensity (MFI) of CD95 expression; (c) percentage of C95L-expressing cells; and (d) the percentage of HLA-DR-expressing cells are shown; (e) percentage of CD95L (■)-expressing cells in B cells.
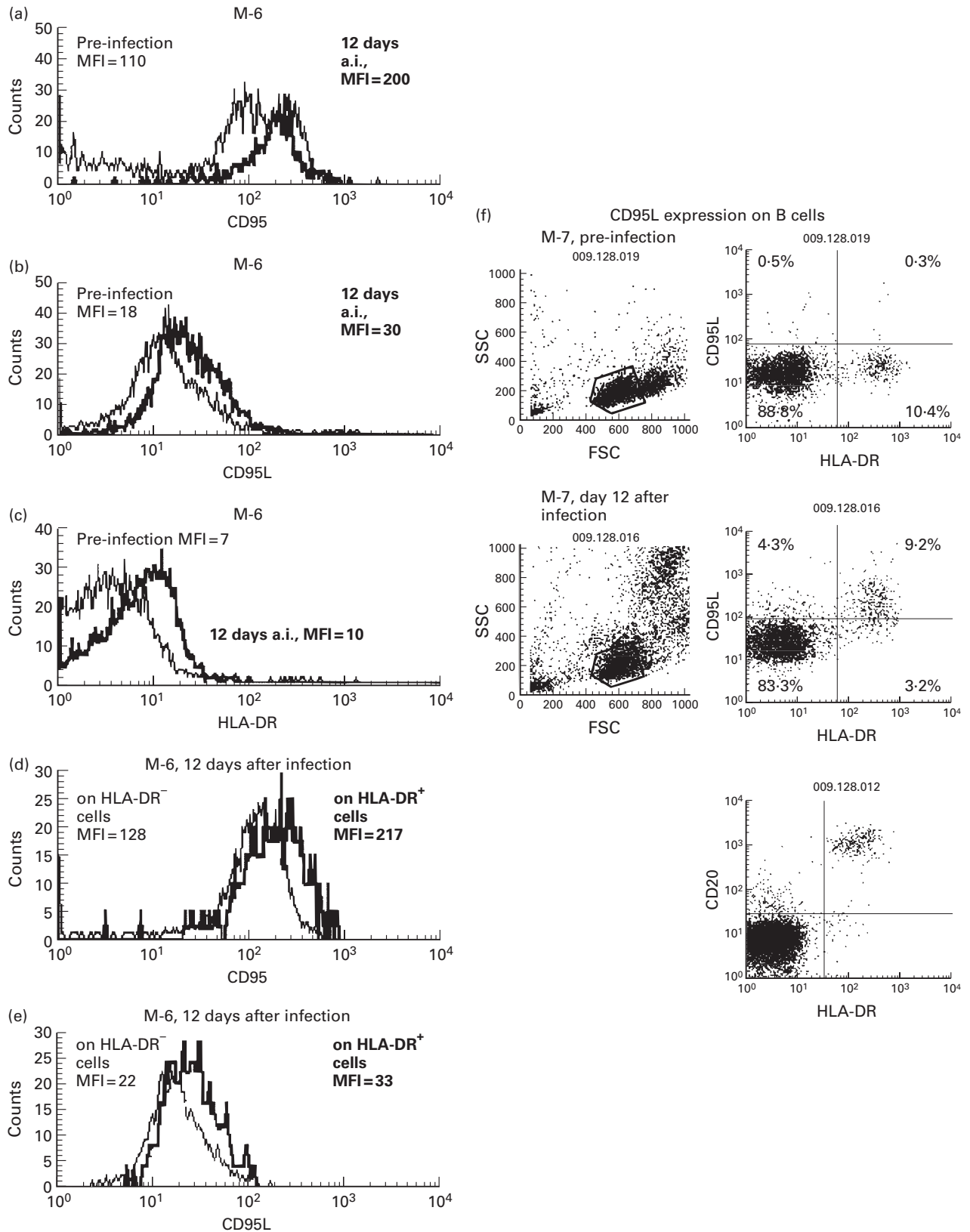
Fig. 4. Images of flow cytometric analysis for CD95, CD95L and HLA-DR expression on lymphocytes. (a) CD95 expression on CD4^{+} cells. (b) CD95L expression on CD8^{+} cells. (c) HLA-DR expression on CD8^{+} cells. (d) CD95 expression on either CD8^{+} HLA-DR^{−} or HLA-DR^{+} cells. (e) CD95L expression on either CD8^{+} HLA-DR^{−} or HLA-DR^{+} cells. (f) CD95L expression on B cells in monkey infected with C2/1. Mean fluorescence intensity (MFI) or percentage of the population is indicated in each histogram or dot image.

virus infection. There is evidence that monocytes induce CD4$^+$ T cell apoptosis since they express CD95L after CD4 cross-linking *in vitro* with gp120 of HIV [26]. In HIV-infected patients however, CD95L expression is down-regulated at the protein level in monocytes [27], although this was not seen in our macaque model.

In conclusion, our newly established macaque model with its rapid CD4$^+$ T lymphocyte loss caused by pathogenic SHIV-C2/1 could be a useful *in vivo* system to assess therapeutic immunomodulators and anti-HIV vaccines.

ACKNOWLEDGMENTS

REFERENCES

1 Ameisen JC, Capron A. Cell dysfunction and depletion in AIDS: the programmed cell death hypothesis. Immunol Today 1991; **12**: 102–5.

2 Gougeon ML, Olivier R, Garcia S, Guetard D, Dragic T, Dauguet C, Montagnier L. Evidence for an engagement process towards cell death by apoptosis in lymphocytes of HIV infected patients. C R Acad Sci III 1991; **312**:529–37.

3 Gougeon ML, Garcia S, Heeney J *et al.* Programmed cell death in AIDS-related HIV and SIV infections. AIDS Res Hum Retrovir 1993; **9**:553–63.

4 Terai C, Kornbluth RS, Pauza CD, Richman DD, Carson DA. Apoptosis as a mechanism of cell death in cultured T lymphoblasts acutely infected with HIV-1. J Clin Invest 1991; **87**:1710–5.

5 Aries SP, Schaaf B, Muller C, Dennin RH, Dalhoff K. Fas (CD95) expression on CD4+ T cells from HIV-infected patients increases with disease progression. L Mol Med 1995; **73**:591–3.

6 Gehri R, Hahn S, Rothem M, Steuerwald M, Nuesch R, Erb P. The Fas receptor in HIV infection: expression on peripheral blood lymphocytes and role in the depletion of T cells. AIDS 1996; **10**:9–16.

7 Gougeon ML, Lecoeur H, Sasaki Y. Apoptosis and the CD95 system in HIV disease. Impact of HAART. Immunol Letters 1999; **66**:97–103.

8 Katsikis PD, Wunderlich ES, Smith CA, Herzenberg LA, Herzenberg LA. Fas antigen stimulation induces marked apoptosis of T lymphocytes in human immunodeficiency virus-infected individuals. J Exp Med 1995; **181**:2029–36.

9 Yonehara S, Ishii A, Yonehara M. A cell-killing monoclonal antibody (anti-Fas) to a cell surface antigen co-downregulated with the receptor of tumor necrosis factor. J Exp Med 1989; **169**:1747–56.

10 Dockrell D, Badley A, Ziesmer S *et al.* Treatment with highly active antiretroviral therapy (HAART) suggests that T cell depletion in HIV-infected individuals correlates with apoptosis mediated by Fas/FasL interaction. 5th Conf Retrovir Oppor Infect 1998:111.

11 Silvestri G, Munoz-Calleja C, Bagnarelli P, Piedimonte G, Clementi M, Montroni M. Early increase of CD4$^+$CD45RA$^+$ and CD4$^+$CD95$^-$ cells with conserved repertoire induced by anti-retroviral therapy in HIV-infected patients. Clin Exp Immunol 1998; **111**:3–11.

12 Noraz N, Gozlan J, Corbeil J, Brunner T, Spector SA. HIV-induced apoptosis of activated primary CD4$^+$ T lymphocytes is not mediated by Fas/Fas ligand. AIDS 1997; **11**:1671–80.

13 Estaquier J, Idziorek T, de Bels F *et al.* Programmed cell death and AIDS. Significance of T-cell apoptosis in pathogenic and nonpathogenic primate lentiviral infections. Proc Natl Acad Sci USA 1994; **91**:9431–5.

14 Iida T, Igarashi T, Ichimura H *et al.* Fas antigen expression and apoptosis of lymphocytes in macaques infected with simian immunodeficiency virus strain mac. Arch Virol 1998; **143**:717–29.

15 Gougeon ML, Lecoeur H, Boudet F *et al.* Lack of chronic immune activation in HIV-infected chimpanzees correlates with the resistance of T cells to Fas/Apo-1 (CD95)-induced apoptosis and preservation of a T helper 1 phenotype. J Immunol 1997; **158**:2964–76.

16 Reinberger S, Spring M, Nisslein T, Stahl-Henning C, Hunsmann G, Dittmer U. Kinetics of lymphocyte apoptosis in macaques infected with different simian immunodeficiency viruses or simian/human immunodeficiency hybrid viruses. Clin Immunol 1999; **90**:141–6.

17 Shinohara K, Sakai K, Ami Y *et al.* A highly pathogenic simian/human immunodeficiency virus with genetic changes in cynomolgus monkey. J Gen Virol 1999; **80**:1231–40.

18 Reimann KA, Li JT, Voss G *et al.* An env gene derived from a primary human immunodeficiency virus type 1 isolate confers high in vivo replicative capacity to a chimeric simian/human immunodeficiency virus in rhesus monkeys. J Virol 1996; **70**:3198–206.

19 Lu Y, Brosio P, Lafaile M, Li J, Collman RG, Sodroski J, Miller CJ. Vaginal transmission of chimeric simian/human immunodeficiency viruses in rhesus macaques. J Virol 1996; **70**:3045–50.

20 Nicoletti I, Migliorati G, Pagliacci MC, Grignani F, Riccardi C. A rapid and simple method for measuring thymocyte apoptosis by propidium iodide staining and flow cytometry. J Immunol Methods 1991; **139**:271–9.

21 Silvestris F, Cafforio P, Frassanito MA, Tucci M, Romito A, Nagata S, Dammacco F. Overexpression of Fas antigen on T cells in advanced HIV-1 infection: differential ligation constantly induces apoptosis. AIDS 1995; **10**:131–41.

22 Haung L, Li CJ, Pardee AB. Human immunodeficiency virus type 1 TAT protein activates B lymphocytes. Biochem Biophys Res Commun 1997; **237**:461–4.

23 Samuelsson A, Sönnerborg A, Heuts N, Cöster J, Chiodi F. Progressive B cell apoptosis and expression of Fas ligand during human immunodeficiency virus type-1 infection. AIDS Res Human Retrovir 1997; **13**:1031–8.

24 Tanner JE, Alfieri C. Epstein-Barr virus induces Fas (CD95) in T cells and Fas ligand in B cells leading to T-cell apoptosis. Blood 1999; **94**:3439–47.

25 Gougeon M-L, Lecoeur H, Dulioust A, Enouf M-G, Crouvoisier M, Goujard C, Debord T, Montagnier L. Programmed cell death in peripheral lymphocytes from HIV-infected persons. J Immunol 1996; **156**:3509–20.

26 Oyaizu N, Adachi Y, Hashimoto F *et al.* Monocytes express Fas ligand upon CD4 cross-linking and induce CD4$^+$ T cell apoptosis. J Immunol 1997; **158**:2456–63.

27 Sieg S, Smith D, Yildirim Z, Kaplan D. Fas ligand deficiency in HIV disease. Proc Natl Acad Sci USA 1997; **94**:5860–5.